Mineralogical Magazine (2022), **86**, 531–538
doi:10.1180/mgm.2021.98

Cambridge University Press

Article

Dendoraite-(NH_4), a new phosphate–oxalate mineral related to thebaite-(NH_4) from the Rowley mine, Arizona, USA

Special Issue dedicated to Peter Williams

Anthony R. Kampf[1]*, Mark A. Cooper[2], Aaron J. Celestian[1], Chi Ma[3] and Joe Marty[1]

[1]Mineral Sciences Department, Natural History Museum of Los Angeles County, 900 Exposition Boulevard, Los Angeles, California 90007, USA; [2]Department of Geological Sciences, University of Manitoba, Winnipeg, Manitoba, R3T 2N2, Canada; and [3]Division of Geological and Planetary Sciences, California Institute of Technology, 1200 East California Boulevard, Pasadena, California 91125, USA

Abstract

Dendoraite-(NH_4), $(NH_4)_2NaAl(C_2O_4)(PO_3OH)_2(H_2O)_2$, is a new mineral species from the Rowley mine, Maricopa County, Arizona, USA. It occurs in an unusual bat-guano-related, post-mining assemblage of phases that include a variety of vanadates, phosphates, oxalates and chlorides, some containing NH_4^+. Other secondary minerals found in association with dendoraite-(NH_4) are antipinite, fluorite, mimetite, mottramite, relianceite-(K), rowleyite, salammoniac, struvite, vanadinite, willemite, wulfenite and at least one other new mineral. Crystals of dendoraite-(NH_4) are colourless blades up to ~0.1 mm in length. The streak is white and lustre is vitreous, Mohs hardness is 2½, tenacity is brittle and fracture is splintery. The calculated density is 2.122 g·cm^{-3}. Dendoraite-(NH_4) is optically biaxial (–) with $\alpha = 1.490(5)$, $\beta = 1.540(5)$ and $\gamma = 1.541(5)$ (white light); $2V_{calc} = 15.7°$; and orientation $X = \mathbf{b}$. Electron microprobe analysis gave the empirical formula $[(NH_4)_{1.48}K_{0.52}]_{\Sigma 2.00}Na_{0.96}(Al_{0.96}Fe^{3+}_{0.03})_{\Sigma 0.99}(C_2O_4)[PO_{2.97}(OH)_{1.03}]_2(H_2O)_2$, with the C, N and H contents constrained by the crystal structure. Dendoraite-(NH_4) is monoclinic, $P2_1/n$, with $a = 10.695(6)$, $b = 6.285(4)$, $c = 19.227(12)$ Å, $\beta = 90.933(10)°$, $V = 1292(2)$ Å^3, and $Z = 4$. The structural unit in the crystal structure of dendoraite-(NH_4) ($R_1 = 0.0467$ for 1322 $I_o > 2\sigma I$ reflections) is a double-strand chain of corner-sharing AlO_6 octahedra and PO_3OH tetrahedra decorated by additional PO_3OH tetrahedra and C_2O_4 groups. Topologically, this is the same chain found in the structure of thebaite-(NH_4). The decorated chains connect to one another through links to $NaO_7(H_2O)$ polyhedra to form a $[Na(H_2O)Al(C_2O_4)(PO_3OH)_2]^{2-}$ sheet, which connect to one another through bonds to (NH_4)/K and through hydrogen bonds.

Keywords: dendoraite-(NH_4), new mineral species, phosphate, oxalate, crystal structure, thebaite-(NH_4), Rowley mine, Arizona

(Received 16 August 2021; accepted 6 December 2021; Accepted Manuscript published online: 13 December 2021; Guest Associate Editor: Clara Magalhães)

Introduction

The still actively forming bat guano assemblage in the Rowley mine in southwestern Arizona, USA, has proven to be a prolific source of new minerals. Including the new mineral described herein, dendoraite-(NH_4), eight new minerals have now been described from this assemblage. Dendoraite-(NH_4), $(NH_4)_2NaAl(C_2O_4)(PO_3OH)_2(H_2O)_2$, is one of only five minerals known to include both phosphate and oxalate groups, the others being davidbrownite-(NH_4), $(NH_4,K)_5(V^{4+}O)_2(C_2O_4)[PO_{2.75}(OH)_{1.25}]_4 \cdot 3H_2O$ (Kampf *et al.*, 2019a), phoxite, $(NH_4)_2Mg_2(C_2O_4)(PO_3OH)_2(H_2O)_4$ (Kampf *et al.*, 2019b), relianceite-(K), $K_4Mg(V^{4+}O)_2(C_2O_4)(PO_3OH)_4(H_2O)_{10}$ (Kampf *et al.*, 2022), and thebaite-(NH_4), $(NH_4,K)_3Al(C_2O_4)(PO_3OH)_2(H_2O)$ (Kampf *et al.*, 2021a); all of these, except phoxite, are known only from the Rowley mine bat guano assemblage. One of these, relianceite-(K), is intimately associated with dendoraite-(NH_4) and is described in a companion paper, Kampf *et al.* (2022).

The name dendoraite is for the Dendora Valley and the Dendora Ranch, which are immediately west of the Rowley mine. For naming and species definition, the total combined occupancy of the two very large cation sites (not the Na site) in the structure is employed; thereby, the '-(NH_4)' suffix in the name reflects the fact that $NH_4^+ > K^+$. If an analogue with $K^+ > NH_4^+$ were found, it would be named 'dendoraite-(K)'.

The new mineral and name were approved by the Commission on New Minerals, Nomenclature and Classification of the International Mineralogical Association (IMA2020-103, Kampf *et al.*, 2021b). The holotype specimen of dendoraite-(NH_4) is deposited in the collections of the Natural History Museum of Los Angeles County, Los Angeles, California, USA, catalogue number 75275. This is also the holotype for relianceite-(K).

Occurrence

Dendoraite-(NH_4) was found on the 125-foot level of the Rowley mine, ~20 km NW of Theba (small settlement and railroad

---

***Author for correspondence:** Anthony R. Kampf, Email: akampf@nhm.org

This paper is part of a thematic set that honours the contributions of Peter Williams

Cite this article: Kampf A.R., Cooper M.A., Celestian A.J., Ma C. and Marty J. (2022) Dendoraite-(NH_4), a new phosphate–oxalate mineral related to thebaite-(NH_4) from the Rowley mine, Arizona, USA. *Mineralogical Magazine* **86**, 531–538. https://doi.org/10.1180/mgm.2021.98

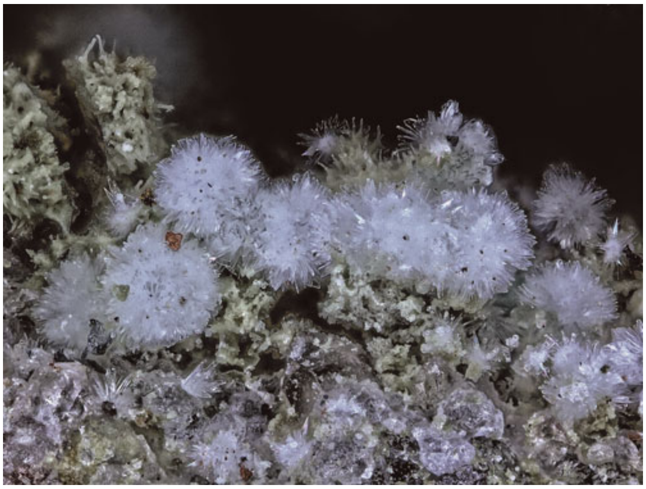

Fig. 1. Sprays of dendoraite-(NH_4) blades; FOV 0.8 mm across; holotype 75275.

depot), Maricopa County, Arizona, USA (33°2'57"N, 113° 1'49.59"W). The Rowley mine is on the western slope of the Painted Rock Mountains (in the Painted Rock mining district) and overlooks the Dendora Valley, immediately to the west. It is a former Cu–Pb–Au–Ag–Mo–V–baryte–fluorspar mine that exploited veins presumed to be related to the intrusion of an andesite porphyry dyke into Tertiary volcanic rocks. Although the mine has not been operated for ore since 1923, collectors took notice of the mine as a source of fine wulfenite crystals around 1945. An up-to-date account of the history, geology, and mineralogy of the mine was recently published by Wilson (2020).

The new mineral was found in a hot and humid area of the mine (see figure 26 in Wilson, 2020) in an unusual bat guano-related, post-mining assemblage of phases that include a variety of vanadates, phosphates, oxalates and chlorides, some containing NH_4^+. This secondary mineral assemblage is found growing on baryte–quartz-rich matrix and, besides dendoraite-(NH_4), includes allantoin (Kampf *et al.*, 2021c), ammineite, antipinite, aphthitalite, bassanite, biphosphammite, cerussite, davidbrownite-(NH_4) (Kampf *et al.*, 2019a), fluorite, halite, hydroglauberite, mimetite, mottramite, natrosulfatourea (Kampf *et al.*, 2021c), perite, phoxite (Kampf *et al.*, 2019b), relianceite-(K) (Kampf *et al.*, 2022), rowleyite (Kampf *et al.*, 2017), salammoniac, struvite, thebaite-(NH_4) (Kampf *et al.*, 2021a), thénardite, urea, vanadinite, weddellite, willemite, wulfenite, and several other potentially new minerals. Dendoraite-(NH_4) was found in intimate association with antipinite, fluorite, mimetite, mottramite, relianceite-(K), rowleyite, salammoniac, struvite, vanadinite, willemite, wulfenite, and at least one other potentially new species.

Physical and optical properties

Crystals of dendoraite-(NH_4) are colourless blades, up to ~0.1 mm in length, generally growing in sprays (Fig. 1). The blades are elongate on [010], flattened on {001}, and taper to a point; the observed crystal forms are {100}, {001}, {310} and {10·1·0} (Fig. 2). No twinning was observed. The streak is white, the lustre is vitreous, the Mohs hardness is ~2½, the tenacity is brittle and the fracture is splintery. No cleavage could be observed with certainty because of the small crystal size; however, the structure suggests two cleavages in the [010] zone, probably perfect on {001} and good on $\{10\bar{1}\}$. The tiny crystals are virtually invisible in density liquids making the measurement of their density impossible. The calculated density is 2.122 g·cm^{-3} using the empirical formula and 2.066 g·cm^{-3} using the ideal (NH_4-end-member) formula. Dendoraite-(NH_4) is non-fluorescent in long- and short-wave ultraviolet light. The mineral is insoluble at room temperature in H_2O, but easily soluble in dilute HCl.

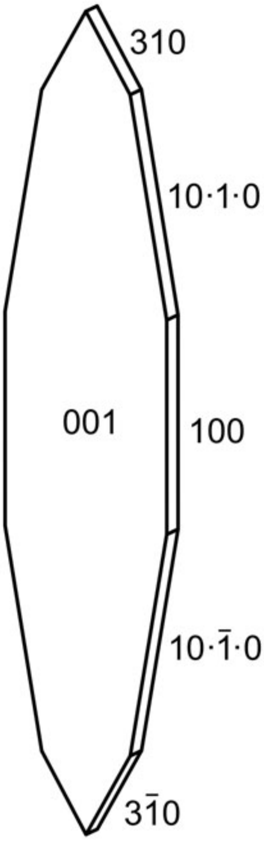

Fig. 2. Crystal drawing of dendoraite-(NH_4); clinographic projection in non-standard orientation, **b** vertical.

Dendoraite-(NH_4) is optically biaxial (–) with $\alpha = 1.490(5)$, $\beta = 1.540(5)$ and $\gamma = 1.541(5)$ determined in white light. The 2V could not be measured because of the small crystal size; the calculated 2V is 15.7°. The partially determined optical orientation is $X = \mathbf{b}$ (length fast). The mineral is non-pleochroic.

Raman spectroscopy

Raman spectroscopy was conducted on a Horiba XploRA PLUS spectrometer using a 532 nm diode laser, 100 µm slit and 1800 gr/mm diffraction grating and a 100× (0.9 NA) objective. Full pattern peak fitting was performed using the least-squares approach using Gaussian peak shapes to minimise the difference between measured and calculated profiles, and cubic-spline was used for base-line modelling. The spectrum from 3800 to 60 cm^{-1} is shown in Fig. 3 including labelled mode assignments based on several references: Frost (2004), Frost *et al.* (2011), Ma and He (2012), Mohaček-Grošev *et al.*, (2009), Rudolph and Irmer

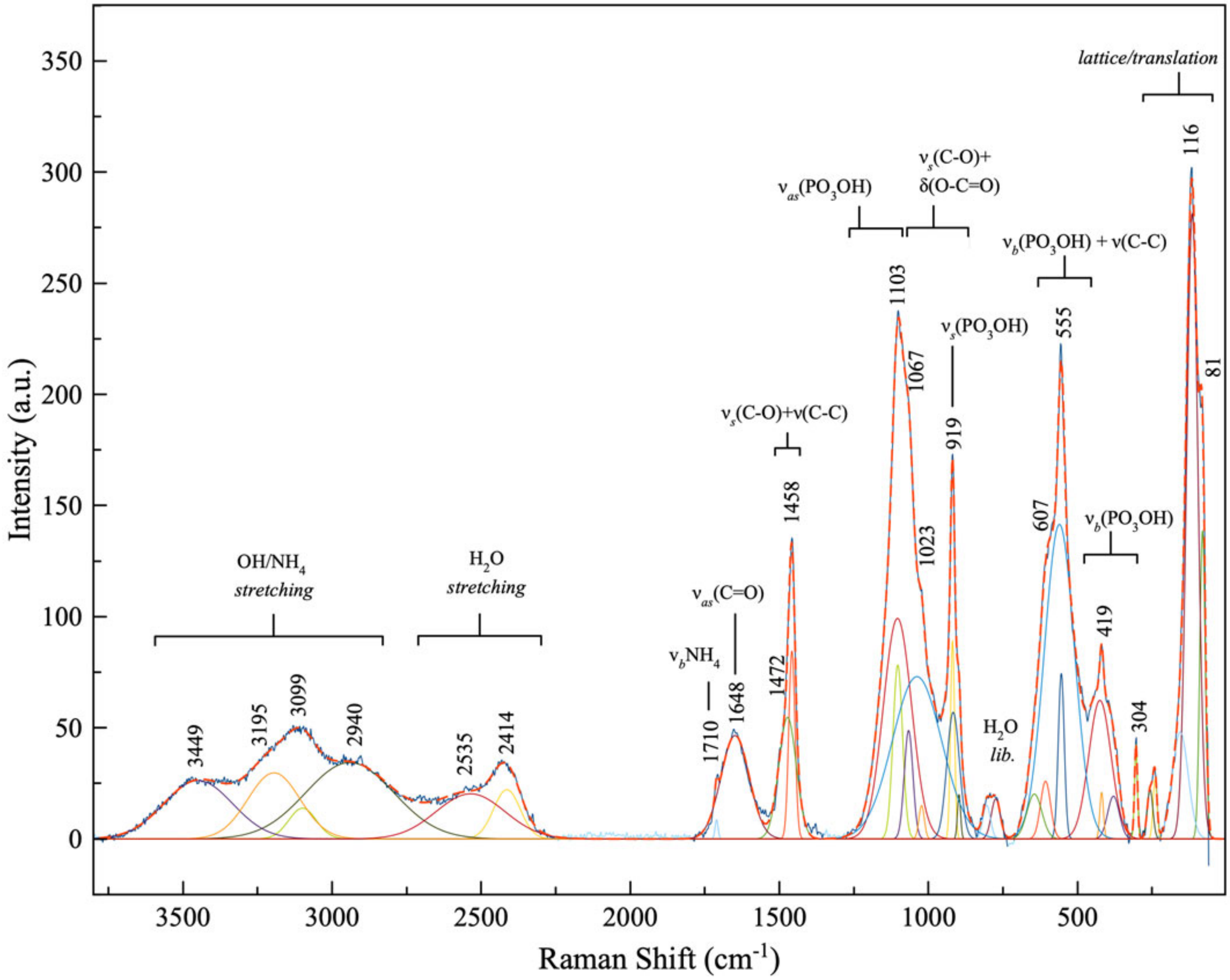

Fig. 3. Raman spectrum of dendoraite-(NH_4).

(2007), Sergeeva *et al.* (2019), Števko *et al.* (2018) and Yakovenchuk *et al.* (2018).

Chemical analysis

Analyses (6 points) were performed at Caltech on a JEOL 8200 electron microprobe in wavelength dispersive spectroscopy mode. Analytical conditions were 15 kV accelerating voltage, 5 nA beam current and 5 µm beam diameter. During vacuum deposition of the conductive carbon coat required for the electron probe microanalysis (EPMA), dendoraite-(NH_4) clearly suffered loss of much of the weakly held H_2O and probably a portion of its NH_4. Dendoraite-(NH_4) was very sensitive to the electron beam and additional loss of these components probably occurred during the EPMA. The very large loss in H_2O resulted in much higher concentrations for the remaining constituents than are to be expected for the fully hydrated phase; therefore, the other analysed constituents have been normalised to provide a total of 100% when combined with the calculated H_2O content. To account for the loss of NH_4, $(NH_4)_2O$ was calculated so that $K + NH_4 = 2$ atoms per formula unit (apfu) in accord with the structure. Insufficient material is available for CHN analysis; however, the fully ordered structure and detailed bond-valence analysis unambiguously established the anion (O, OH, H_2O and C_2O_4) identities and the corresponding quantitative contents of H_2O and CO_2. Analytical data are given in Table 1.

Table 1. Analytical data (wt.%) for dendoraite-(NH_4).

Constituent	Mean	Min.	Max.	S.D.	Probe standard	Normalised
$(NH_4)_2O$*	6.03	5.12	7.14	0.86	BN	9.31
K_2O	6.53	6.05	7.18	0.38	microcline	5.95
Na_2O	7.88	6.83	8.68	0.68	albite	7.18
Al_2O_3	13.02	12.92	13.15	0.08	sanidine	11.87
Fe_2O_3	0.71	0.62	0.84	0.08	fayalite	0.65
P_2O_5	37.72	37.33	38.23	0.38	apatite	34.38
C_2O_3*						17.44
H_2O*						13.22
Total						100.00

* $(NH_4)_2O$, C_2O_3 and H_2O values in the Normalised column are based on the structure.

The empirical formula (based on P = 2 and O = 14 apfu) is $[(NH_4)_{1.48}K_{0.52}]_{\Sigma 2.00}Na_{0.96}(Al_{0.96}Fe^{3+}_{0.03})_{\Sigma 0.99}(C_2O_4)[PO_{2.97}(OH)_{1.03}]_2$

Table 2. Powder X-ray data (d in Å) for dendoraite-(NH_4).

I_{obs}	d_{obs}	d_{calc}	I_{calc}	hkl	I_{obs}	d_{obs}	d_{calc}	I_{calc}	hkl
100	9.65	9.6122	100	0 0 2	6	2.554	2.5593	2	$\bar{1}$ 2 4
54	9.29	9.2811	76	1 0 1			2.5488	6	1 2 4
24	5.99	5.9739	15	0 1 1	6	2.505	2.5028	5	$\bar{2}$ 2 3
23	5.41	5.4184	11	1 1 0	19	2.449	2.4579	7	$\bar{1}$ 1 7
		5.2603	2	0 1 2			2.4415	3	1 1 7
9	4.894	4.8061	7	0 0 4			2.4356	3	4 1 1
28	4.738	4.7369	5	$\bar{1}$ 1 2			2.4332	2	0 2 5
		4.7036	15	1 1 2			2.4305	2	$\bar{3}$ 1 5
8	4.490	4.4871	2	0 1 3	6	2.389	2.3919	3	$\bar{4}$ 1 2
20	4.153	4.1545	6	$\bar{1}$ 1 3			2.3083	2	$\bar{4}$ 1 3
		4.0725	3	2 1 0	11	2.234	2.2446	5	0 1 8
18	3.612	3.6370	5	$\bar{1}$ 0 5			2.2233	4	$\bar{2}$ 2 5
		3.5995	11	1 0 5	12	2.192	2.2035	4	$\bar{1}$ 1 8
5	3.552	3.5458	3	2 0 4			2.1907	2	1 2 6
		3.5151	5	$\bar{3}$ 0 1			2.1786	4	2 0 8
40	3.455	3.4566	26	$\bar{2}$ 1 3	8	2.129	2.1294	6	$\bar{5}$ 0 1
		3.4180	13	2 1 3	9	2.060	2.0585	2	2 1 8
8	3.207	3.2041	12	0 0 6			2.0469	2	0 3 2
		3.1425	2	0 2 0			2.0449	2	$\bar{1}$ 3 1
		3.1368	2	$\bar{3}$ 0 3	19	2.034	2.0387	2	$\bar{5}$ 0 3
		3.1235	2	1 1 5			2.0365	2	4 0 6
75	3.106	3.1013	38	0 2 1			2.0275	6	$\bar{4}$ 2 1
		3.0937	17	3 0 3			2.0247	2	5 1 0
		3.0150	4	1 2 0	5	1.9438	1.9367	2	$\bar{2}$ 2 7
		2.9869	2	0 2 2	8	1.8991	1.9086	2	$\bar{3}$ 2 6
		2.9807	2	$\bar{1}$ 2 1	8	1.8101	1.8192	2	3 0 9
28	2.975	2.9765	5	1 2 1			1.8165	2	$\bar{1}$ 1 10
		2.9631	18	$\bar{3}$ 1 2			1.7996	2	$\bar{3}$ 3 1
		2.8806	2	$\bar{1}$ 2 2	8	1.7655	1.7729	2	4 0 8
33	2.825	2.8215	20	0 2 3			1.7666	3	0 2 9
		2.8067	4	$\bar{3}$ 1 3			1.7575	2	$\bar{6}$ 0 2
		2.7683	2	$\bar{2}$ 0 6	6	1.7278	1.7203	3	1 0 11
19	2.729	2.7289	10	2 0 6	4	1.7023	1.7055	2	6 1 1
		2.7233	4	1 2 3	15	1.6673	1.6707	5	2 2 9
		2.7092	3	2 2 0			1.6629	4	$\bar{6}$ 1 3
		2.6858	2	$\bar{2}$ 2 1	10	1.6352	1.6400	2	$\bar{3}$ 3 5
		2.6797	2	2 2 1	7	1.5699	1.5713	2	0 4 0
14	2.668	2.6734	6	4 0 0			1.5507	2	0 4 2
		2.6497	7	1 0 7	7	1.5342	1.5329	2	1 1 12
10	2.639	2.6355	7	$\bar{3}$ 0 5			1.5260	2	0 4 3

Table 3. Data collection and structure refinement details for dendoraite-(NH_4).

Crystal Data	
Refined formula	$[(NH_4)_{1.314}K_{0.686}]Na(Al_{0.916}Fe_{0.084})(C_2O_4)(PO_3OH)_2(H_2O)_2$
Space group	$P2_1/n$
Unit cell dimensions	a = 10.695(6) Å b = 6.285(4) Å c = 19.227(12) Å β = 90.933(10)°
V	1292.2(14) Å^3
Z	4
Density (calculated) (g·cm^{-3})	2.118
Absorption coefficient (mm^{-1})	0.841
F(000)	822.1
Data Collection	
Diffractometer	Bruker D8 three-circle; multilayer optics; APEX-II CCD
X-ray radiation / source	Mo*K*α (λ = 0.71073 Å) / rotating anode
Temperature (K)	293(2)
Crystal size (μm)	50 × 20 × 4
θ range for data collection (°)	2.16 to 22.67.
Index ranges	$-11 \le h \le 11$, $-6 \le k \le 6$, $-20 \le l \le 20$
Reflections collected	6348
Independent reflections	1695 [$R_{int} = 0.070$]
Reflections with $I_o > 2\sigma I$	1322
Completeness to θ = 22.67°	98.0%
Refinement	
Refinement method	Full-matrix least-squares on F^2
Parameters / restraints	215 / 4
Goodness-of-fit on F^2	1.066
Final R indices [$I > 2\sigma(I)$]	$R_1 = 0.0467$, $wR_2 = 0.1118$
R indices (all data)	$R_1 = 0.0649$, $wR_2 = 0.1207$
$\Delta\rho_{max}$, $\Delta\rho_{min}$ (e^-/A^3)	0.42 and –0.33

*$R_{int} = \Sigma|F_o^2 - F_o^2(\text{mean})|/\Sigma[F_o^2]$. GoF = $S = \{\Sigma[w(F_o^2 - F_c^2)^2]/(n-p)\}^{½}$. $R_1 = \Sigma||F_o| - |F_c||/\Sigma|F_o|$. $wR_2 = \{\Sigma[w(F_o^2 - F_c^2)^2]/\Sigma[w(F_o^2)^2]\}^{½}$; $w = 1/[\sigma^2(F_o^2) + (aP)^2 + bP]$ where a is 0.0601, b is 2.3477 and P is $[2F_c^2 + \text{Max}(F_o^2,0)]/3$.

$(H_2O)_2$. The simplified formula is $(NH_4,K)_2Na(Al,Fe^{3+})(C_2O_4)(PO_3OH)_2(H_2O)_2$ and the ideal (NH_4-end-member) formula is $(NH_4)_2NaAl(C_2O_4)(PO_3OH)_2(H_2O)_2$ which requires $(NH_4)_2O$ 12.95, Na_2O 7.71, Al_2O_3 12.68, P_2O_5 35.30, C_2O_3 17.91, H_2O 13.44, total 100 wt.%. The Gladstone–Dale compatibility (Mandarino, 2007) 1 – (K_p/K_c) is 0.018 in the range of superior compatibility for the empirical formula.

X-ray crystallography and structure determination

Powder X-ray studies were done using a Rigaku R-Axis Rapid II curved imaging plate microdiffractometer with monochromatised Mo*K*α radiation. A Gandolfi-like motion on the φ and ω axes was used to randomise the sample. Observed d values and intensities were derived by profile fitting using *JADE Pro* software (Materials Data, Inc., USA). The powder data are presented in Table 2. Unit-cell parameters refined from the powder data using *JADE Pro* with whole pattern fitting are a = 10.702(7), b = 6.289(7), c = 19.236(7) Å, β = 90.961(14)°, and V = 1294.5(17) Å^3.

Single-crystal X-ray studies were done using a Bruker D8 three-circle diffractometer equipped with a rotating anode generator (Mo*K*α X-radiation), multilayer optics and an APEX-II CCD area detector. A total of 22,987 reflections were integrated from 94 s frames with a 0.3° frame width. The unit-cell dimensions were obtained by least-squares refinement of 2770 reflections with $I_o > 8\sigma I$. Empirical absorption corrections (*SADABS; Sheldrick, 2015*) were applied and equivalent reflections were merged. Systematically absent reflections are consistent with space group $P2_1/n$ and the structure was successfully solved in that space group by direct methods using *SHELXS-2013*. The structure was refined using *SHELXL-2016* (Sheldrick, 2015). Two large-cation sites were refined with joint occupancies by N and K, showing both to have N(NH_4) > K. A somewhat smaller cation site was consistent with full occupancy by Na. Al was assigned to a small octahedrally coordinated cation site, but exhibited a slight excess of scattering power indicating a small Fe content; the site was ultimately refined with joint Al/Fe occupancy. Difference-Fourier syntheses located all H atom sites except those associated with the two N/K sites and with the OW2 site. Note that one possible H site associated with OW2 was indicated in the difference Fourier; however, a second H site was not apparent and, because of the strongly prolate nature of the OW2 site, we lack confidence in assigning any H sites for OW2. The H sites associated with OH1, OH5 and OW1 were refined with restraints of 0.98(1) Å on the O–H distances. Data collection and refinement details are given in Table 3, atom coordinates and displacement parameters in Table 4, selected bond distances in Table 5 and a bond-valence analysis in Table 6. The crystallographic information files have been deposited with the Principal Editor of *Mineralogical Magazine* and are available as Supplementary material (see below).

Table 4. Atom positions, occupancy and displacement parameters (Å)^2 for dendoraite-(NH_4).

	Occupancy	*x*/*a*	*y*/*b*	*z*/*c*	U^{11}	U^{22}	U^{33}	U^{23}	U^{13}	U^{12}	U_{eq}
Al	$Al_{0.916}Fe_{0.084(6)}$	0.92475(12)	0.4076(2)	0.22151(7)	0.0110(8)	0.0139(9)	0.0230(9)	0.0002(6)	0.0011(5)	0.0002(6)	0.0159(6)
P1	P	0.62615(11)	0.4102(2)	0.24790(7)	0.0114(7)	0.0153(7)	0.0236(8)	−0.0010(6)	0.0007(5)	−0.0006(6)	0.0168(4)
P2	P	0.84828(13)	0.5461(2)	0.06720(7)	0.0230(8)	0.0237(8)	0.0242(8)	0.0023(6)	0.0003(6)	−0.0026(6)	0.0236(4)
C1	C	0.6132(5)	0.1277(9)	0.8183(3)	0.023(3)	0.024(3)	0.029(3)	0.000(2)	−0.004(3)	0.001(2)	0.0254(13)
C2	C	0.6772(5)	0.1104(8)	0.7472(3)	0.020(3)	0.012(3)	0.039(3)	0.003(2)	0.000(3)	0.001(2)	0.0236(13)
Na	Na	0.90765(19)	0.1683(4)	0.85151(11)	0.0225(12)	0.0477(15)	0.0318(13)	0.0058(10)	0.0000(9)	−0.0097(11)	0.0340(6)
N1	$N_{0.544}K_{0.456(10)}$	0.7137(2)	0.0567(4)	0.09894(14)	0.059(2)	0.0344(17)	0.062(2)	−0.0044(12)	0.0066(13)	−0.0034(12)	0.0517(13)
N2	$N_{0.770}K_{0.230(11)}$	0.3402(4)	0.3561(7)	0.0980(2)	0.065(3)	0.070(3)	0.073(3)	−0.003(2)	−0.009(2)	0.001(2)	0.070(2)
OH1	OH	0.5947(3)	0.4099(6)	0.16733(18)	0.022(2)	0.025(2)	0.028(2)	0.0002(17)	−0.0029(16)	−0.0017(17)	0.0250(9)
H1	H	0.649(4)	0.485(8)	0.135(2)							0.078(12)
O2	O	0.5673(3)	0.6027(5)	0.28226(17)	0.0163(19)	0.018(2)	0.030(2)	−0.0009(16)	0.0034(15)	−0.0009(15)	0.0212(8)
O3	O	0.7674(3)	0.4103(5)	0.25843(18)	0.0110(18)	0.022(2)	0.031(2)	0.0021(16)	0.0005(15)	0.0003(15)	0.0213(8)
O4	O	0.5668(3)	0.2122(5)	0.27707(17)	0.0130(18)	0.0149(19)	0.031(2)	0.0017(15)	0.0040(14)	0.0002(15)	0.0195(8)
OH5	OH	0.8370(3)	0.3967(6)	0.00002(19)	0.033(2)	0.036(2)	0.028(2)	−0.0069(18)	−0.0004(17)	−0.0066(19)	0.0324(10)
H2	H	0.916(3)	0.341(9)	−0.018(3)							0.078(12)
O6	O	0.9485(3)	0.7111(6)	0.05516(19)	0.032(2)	0.030(2)	0.033(2)	0.0009(18)	0.0031(18)	−0.0124(19)	0.0319(10)
O7	O	0.8835(3)	0.3977(5)	0.12716(17)	0.022(2)	0.025(2)	0.024(2)	0.0011(16)	−0.0027(15)	−0.0011(16)	0.0235(9)
O8	O	0.7193(3)	0.6363(6)	0.0760(2)	0.027(2)	0.032(2)	0.041(2)	0.0040(18)	−0.0013(17)	0.0041(18)	0.0335(10)
O9	O	0.4963(3)	0.1019(6)	0.81543(18)	0.016(2)	0.031(2)	0.027(2)	−0.0016(17)	0.0002(15)	0.0002(17)	0.0246(9)
O10	O	0.6775(4)	0.1641(7)	0.8712(2)	0.027(2)	0.062(3)	0.036(3)	−0.001(2)	−0.010(2)	−0.003(2)	0.0418(11)
O11	O	0.6015(3)	0.0838(5)	0.69642(18)	0.0180(19)	0.022(2)	0.026(2)	0.0000(16)	0.0001(16)	−0.0030(17)	0.0221(9)
O12	O	0.7924(3)	0.1193(7)	0.7436(2)	0.014(2)	0.046(3)	0.046(3)	−0.004(2)	0.0003(17)	−0.0004(18)	0.0353(10)
OW1	H_2O	0.1088(4)	0.1313(7)	0.0771(2)	0.051(3)	0.037(3)	0.039(3)	0.002(2)	0.006(2)	0.005(2)	0.0423(11)
H3	H	0.088(6)	0.155(11)	0.0279(9)							0.078(12)
H4	H	0.044(3)	0.198(8)	0.105(2)							0.078(12)
OW2	H_2O	0.5239(6)	0.2473(12)	0.9864(3)	0.091(5)	0.133(7)	0.077(4)	−0.018(4)	0.015(4)	−0.012(4)	0.100(2)

Discussion of the structure

The N1 and N2 sites are both ten-fold coordinated, the Na site is seven-fold coordinated. The Al site is octahedrally coordinated and two P sites, P1 and P2, are both tetrahedrally coordinated by three O and one OH. One oxalate (C_2O_4) group includes two independent C sites, C1 and C2, and four independent O sites.

Table 5. Selected bond lengths (Å) and angles (°) for dendoraite-(NH_4).

Al–O3	1.838(4)	P1–O4	1.509(4)	P2–O8	1.504(4)
Al–O7	1.861(4)	P1–O2	1.520(4)	P2–O6	1.512(4)
Al–O4	1.917(4)	P1–O3	1.521(4)	P2–O7	1.525(4)
Al–O2	1.920(4)	P1–OH1	1.580(4)	P2–OH5	1.600(4)
Al–O9	1.951(4)	<P1–O>	1.533	<P2–O>	1.535
Al–O11	1.960(4)				
<Al–O>	1.908	N1–O8	2.679(5)	N2–O12	2.858(6)
		N1–O7	2.856(4)	N2–OW1	2.873(6)
C1–C2	1.544(8)	N1–OH1	2.887(5)	N2–OW2	3.010(7)
C1–O9	1.261(6)	N1–O3	2.896(5)	N2–OH1	3.030(5)
C1–O10	1.240(6)	N1–O9	2.978(4)	N2–OH5	3.073(6)
C2–O11	1.268(6)	N1–OH5	3.164(5)	N2–O10	3.080(6)
C2–O12	1.237(6)	N1–OW2	3.178(8)	N2–O11	3.224(6)
		N1–O2	3.257(5)	N2–OW2	3.323(8)
Na–OW1	2.338(5)	N1–O6	3.435(5)	N2–O10	3.328(7)
Na–O4	2.364(4)	N1–OW2	3.558(7)	N2–O8	3.396(6)
Na–O12	2.416(5)	<N1–O>	3.089	<N2–O>	3.120
Na–O6	2.464(4)				
Na–O10	2.497(5)				
Na–O2	2.768(4)				
Na–O11	2.771(4)				
<Na–O>	2.517				

Hydrogen bonds	$O_D\cdots O_A$	$H\cdots O_A$	$O_D–H\cdots O_A$	$O_A–O_D–O_A$
OH1–H1···O8	2.638(5)	1.668(14)	170(7)	
OH5–H2···O6	2.632(5)	1.661(15)	170(7)	
OW1–H3···O6	2.788(6)	1.84(3)	162(7)	
OW1–H4···O7	3.100(5)	2.18(3)	157(6)	
O6–OW1–O7				86.04(15)
OW2···O10	2.828(7)			
OW2···O8	2.938(8)			
O10–OW2–O8				104.3(2)

The structural unit is a double-strand chain of corner-sharing AlO_6 octahedra and $P1O_3OH$ tetrahedra decorated by $P2O_3OH$ tetrahedra and C_2O_4 groups. This decorated $[Al(C_2O_4)(PO_3OH)_2]^{3-}$ chain is topologically identical to that in thebaite-(NH_4), although the $P2O_3OH$ tetrahedra have distinctly different orientations in the two structures (Fig. 4). Without the decorating $P2O_3OH$ tetrahedra and C_2O_4 groups, this octahedral–tetrahedral double-strand chain is topologically identical to the chain in hannayite, $Mg_3(NH_4)_2(HPO_4)_4{\cdot}8H_2O$ (Catti and Franchini-Angela, 1976), while those in galliskiite, $Ca_4Al_2(PO_4)_2F_8{\cdot}5H_2O$ (Kampf *et al.*, 2010) and kapundaite, $(Na,Ca)_2Fe_4^{3+}(PO_4)_4(OH)_3{\cdot}5H_2O$ (Mills *et al.*, 2010) are geometrical isomers.

The chains in the structure of dendoraite-(NH_4) are linked to one another through $NaO_7(H_2O)$ polyhedra. Each Na-centred polyhedron shares an edge with a $P1O_3OH$ tetrahedron, an edge with an AlO_6 octahedron and a corner with a $P2O_3OH$ tetrahedron, all in the same chain. Another edge of the $NaO_7(H_2O)$ polyhedron links to an adjacent chain *via* the bridging C_2O_4 group. In this manner, the chains are joined to form a $[Na(H_2O)Al(C_2O_4)(PO_3OH)_2]^{2-}$ sheet parallel to {001} (Fig. 5). The region between the sheets contains the two (NH_4)/K sites, N1 and N2, and an H_2O group, OW2, that bonds to both (NH_4)/K sites. The $[Na(H_2O)Al(C_2O_4)(PO_3OH)_2]^{2-}$ sheets connect to one another through bonds to (NH_4)/K and through hydrogen bonds (Fig. 6).

As already shown, the $[AlC_2O_4(PO_3OH)_2]^{3-}$ chains in dendoraite-(NH_4) and thebaite-(NH_4) are very similar. The P1 and P2 tetrahedra are $PO_3(OH)$ groups delivering strong intra- and inter-chain H-bonds (i.e. $OH\cdots O_A$ distances are 2.59–2.64 Å). Both structures contain similar intra-chain H-bonds directed from

Table 6. Bond-valence analysis for dendoraite-(NH_4). Values are in valence units (*vu*).

	Al	P1	P2	C1	C2	Na	N1	N2	Hydrogen bonds		Σ
									donated	accepted	
OH1		1.12					0.15	0.11	−0.26		1.12
O2	0.48	1.30				0.08	0.06				1.92
O3	0.59	1.29					0.14				2.02
O4	0.48	1.33				0.20					2.01
OH5			1.06				0.07	0.10	−0.27		0.96
O6			1.32			0.16	0.03			0.27, 0.19	1.97
O7	0.56		1.28				0.16			0.11	2.11
O8			1.35				0.25	0.04		0.26, 0.14	2.05
O9	0.44			1.41			0.12				1.97
O10				1.49		0.15		0.09, 0.05		0.17	1.96
O11	0.43				1.39	0.08		0.06			1.96
O12					1.50	0.18		0.17			1.85
OW1						0.22		0.16	−0.19, −0.11		0.08
OW2							0.07, 0.03	0.11, 0.05	−0.17, −0.14		−0.06
Σ	2.98	5.04	5.01	2.90	2.89	1.07	1.07	0.94			

Bond-valence parameters for NH_4^+–O are from Garcia-Rodriguez *et al.* (2000); all others are from Gagné and Hawthorne (2015). The K/N sites were modelled using refined occupancies. Hydrogen-bond strengths are based on O–O distances according to the relation of Ferraris and Ivaldi (1988).

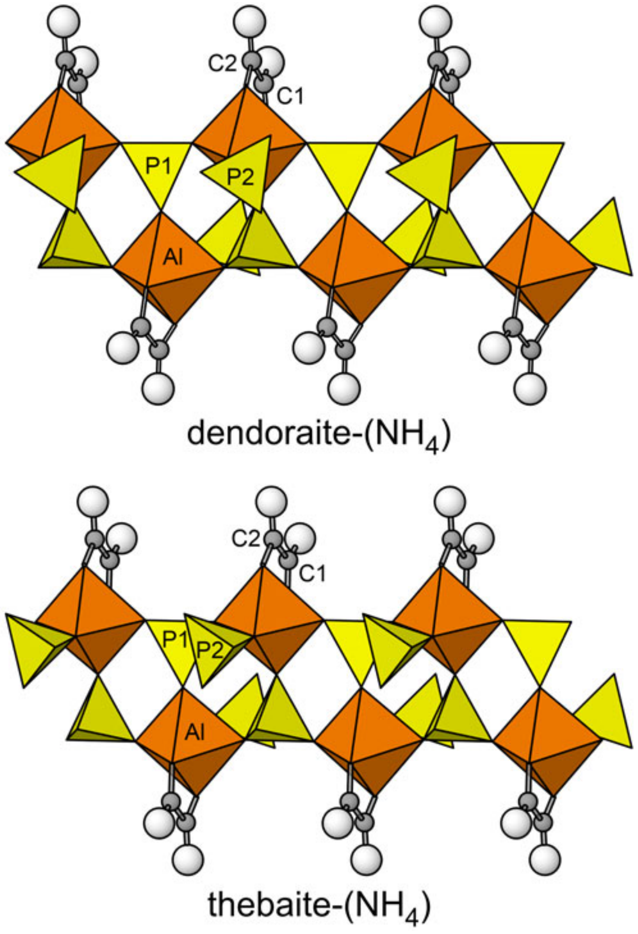

Fig. 4. The chains along [010] in the structures of dendoraite-(NH_4) and thebaite-(NH_4). [100] is vertical; [010] is canted down 20° from right to left.

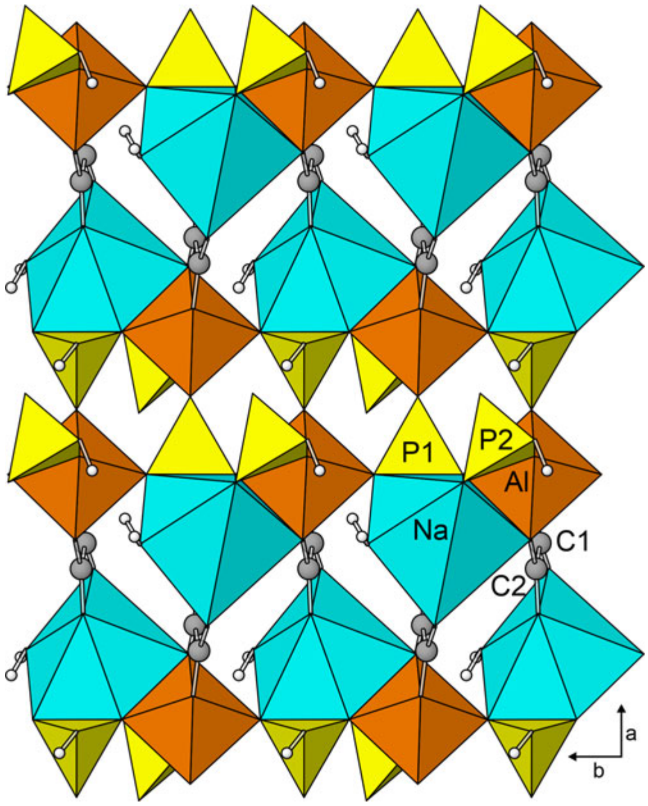

Fig. 5. The sheet parallel to {001} in the structure of dendoraite-(NH_4).

the OH group at OH1 of the P1 tetrahedron towards an O^{2-} anion of the decorating P2 tetrahedron. However, the two structures differ in their inter-chain H-bond that is directed from the OH group at OH5 of the P2 tetrahedron to an O^{2-} anion of the neighbouring chain. In dendoraite-(NH_4), this inter-chain H-bond is directed towards an O^{2-} anion of a P2 tetrahedron of the neighbouring chain, whereas in thebaite-(NH_4) it is directed towards an O^{2-} anion of the C_2O_4 group of the neighbouring chain. This difference in H-bond linkage between $[AlC_2O_4(PO_3OH)_2]^{3-}$ chains in the two structures is facilitated by a relative ~180° rotation of half of the P2 tetrahedra, and lateral offset between chains within the {010} plane (Fig. 7).

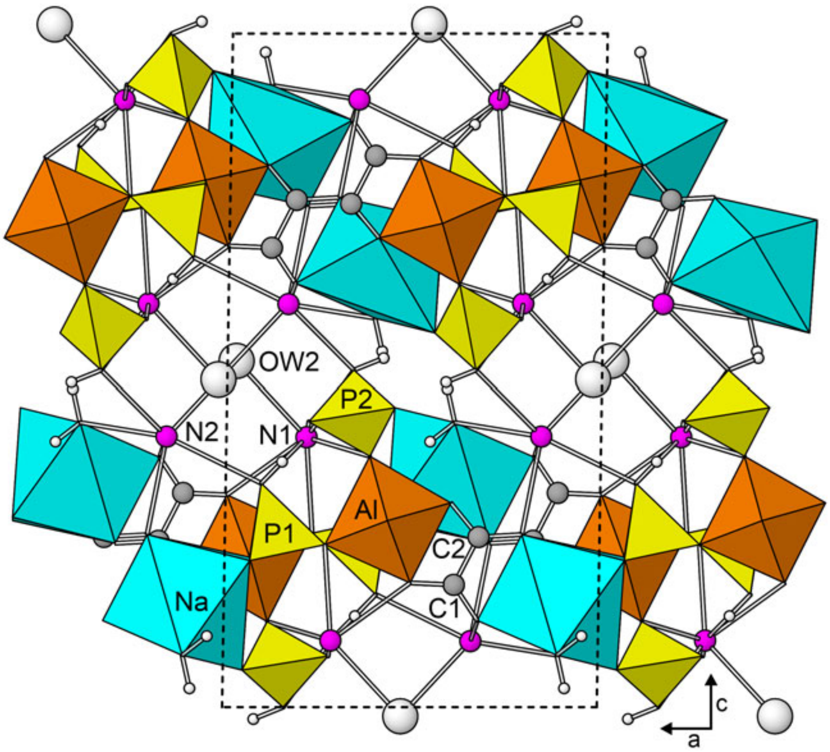

Fig. 6. The dendoraite-(NH_4) structure viewed down [010]. The unit cell outline is shown with dashed lines.

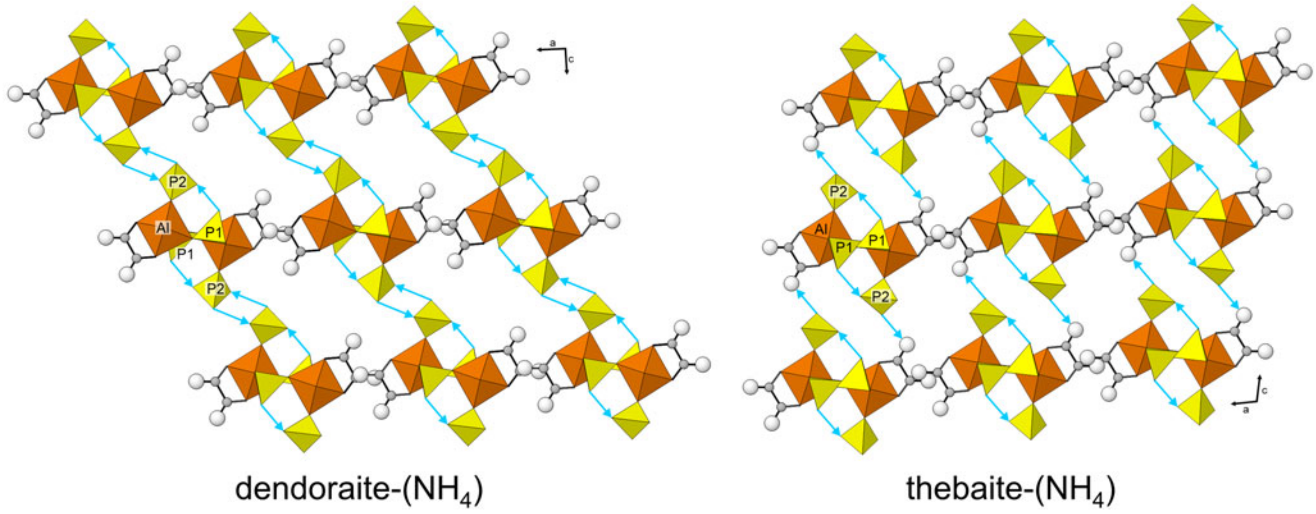

dendoraite-(NH_4)

thebaite-(NH_4)

Fig. 7. Hydrogen-bond linkages between the $[AlC_2O_4(PO_3OH)_2]^{3-}$ chains in the structures of dendoraite-(NH_4) and thebaite-(NH_4) viewed down [010]. The hydrogen bonds are shown as turquoise-coloured lines pointing from the donating OH group toward the receiving O atom.

Acknowledgements. Anonymous reviewers and Pete Leverett are thanked for constructive comments, which improved the manuscript. Keith Wentz, claim holder of the Rowley mine, is thanked for allowing underground access for the study of the occurrence and the collecting of specimens, along with Frank Hawthorne for providing access to the single-crystal instrument at the University of Manitoba. This study was funded, in part, by the John Jago Trelawney Endowment to the Mineral Sciences Department of the Natural History Museum of Los Angeles County.

Supplementary material.. To view supplementary material for this article, please visit https://doi.org/10.1180/mgm.2021.98

References

Catti M. and Franchini-Angela M. (1976) Hydrogen bonding in the crystalline state. Structure of $Mg_3(NH_4)_2(HPO_4)_4(H_2O)_8$ (hannayite), and crystal chemical relationships with schertelite and struvite. *Acta Crystallographica*, **B32**, 2842–2848.

Ferraris G. and Ivaldi G. (1988) Bond valence vs. bond length in O···O hydrogen bonds. *Acta Crystallographica*, **B44**, 341–344.

Frost R.L. (2004) Raman spectroscopy of natural oxalates. *Analytica Chimica Acta*, **517**, 207–214.

Frost R.L., Palmer S.J. and Pogson R.E. (2011) Raman spectroscopy of newberyite $Mg(PO_3OH)\cdot 3H_2O$: A cave mineral. *Spectrochimica Acta Part A: Molecular and Biomolecular Spectroscopy*, **79**, 1149–1153.

Gagné O.C. and Hawthorne F.C (2015) Comprehensive derivation of bond-valence parameters for ion pairs involving oxygen. *Acta Crystallographica*, **B71**, 562–578.

García-Rodríguez L., Rute-Pérez Á., Piñero J.R. and González-Silgo C. (2000) Bond-valence parameters for ammonium-anion interactions. *Acta Crystallographica*, **B56**, 565–569.

Kampf A.R., Colombo F., Simmons W.B., Falster A.U., and Nizamoff J.W. (2010) Galliskiite, $\mathrm{Ca_4Al_2(PO_4)_2F_8 \cdot 5H_2O}$, a new mineral from the Gigante granitic pegmatite, Córdoba province, Argentina. *American Mineralogist*, **95**, 392–396.

Kampf A.R., Cooper M.A., Nash B.P., Cerling T., Marty J., Hummer D.R., Celestian A.J., Rose T.P. and Trebisky T.J. (2017) Rowleyite, $[\mathrm{Na(NH_4,K)_9Cl_4}][\mathrm{V_2^{5+,4+}(P,As)O_8}]_6 \cdot n[\mathrm{H_2O,Na,NH_4,K,Cl}]$, a new mineral with a mesoporous framework structure. *American Mineralogist*, **102**, 1037–1044.

Kampf A.R., Cooper M.A., Rossman R.R., Nash B.P., Hawthorne F.C. and Marty J. (2019a) Davidbrownite-($\mathrm{NH_4}$), $\mathrm{(NH_4,K)_5(V^{4+}O)_2(C_2O_4)[PO_{2.75}(OH)_{1.25}]_4 \cdot 3H_2O}$, a new phosphate–oxalate mineral from the Rowley mine, Arizona, USA. *Mineralogical Magazine*, **83**, 869–877.

Kampf A.R., Celestian A.J., Nash B.P. and Marty J. (2019b) Phoxite, $\mathrm{(NH_4)_2Mg_2(C_2O_4)(PO_3OH)_2(H_2O)_4}$, the first phosphate–oxalate mineral. *American Mineralogist*, **104**, 973–979.

Kampf A.R., Cooper M.A., Celestian A.J., Nash B.P. and Marty J. (2021a) Thebaite-($\mathrm{NH_4}$), $\mathrm{(NH_4,K)_3Al(C_2O_4)(PO_3OH)_2(H_2O)}$, a new phosphate–oxalate mineral from the Rowley mine, Arizona, USA. *Mineralogical Magazine*, **85**, 379–386.

Kampf A.R., Cooper M.A., Celestian A.J., Ma C. and Marty J. (2021b) Dendoraite-(NH4), IMA 2020-103. CNMNC Newsletter 61; *Mineralogical Magazine*, **85**, https://doi.org/10.1180/mgm.2021.48

Kampf A.R., Celestian A.J., Nash B.P. and Marty J. (2021c) Allantoin and natrosulfatourea, two new bat-guano minerals from the Rowley mine, Maricopa County, Arizona, U.S.A. *The Canadian Mineralogist*, **59**, 603–616.

Kampf A.R., Cooper M.A., Celestian A., Ma C. and Marty J. (2022) Relianceite-(K), a new phosphate-oxalate mineral related to davidbrownite-($\mathrm{NH_4}$) from the Rowley mine, Arizona, USA. *Mineralogical Magazine*, **86**, https://doi.org/10.1180/mgm.2021.99.

Ma Q. and He H. (2012) Synergistic effect in the humidifying process of atmospheric relevant calcium nitrate, calcite and oxalic acid mixtures. *Atmospheric Environment*, **50**, 97–102.

Mandarino J.A. (2007) The Gladstone–Dale compatibility of minerals and its use in selecting mineral species for further study. *The Canadian Mineralogist*, **45**, 1307–1324.

Mills S.J., Birch W.D., Kampf A.R., Christy A. G., Pluth J.J., Pring A., Raudsepp M. and Chen Y. (2010) Kapundaite, $\mathrm{(Na,Ca)_2Fe_4^{3+}(PO_4)_4(OH)_3 \cdot 5H_2O}$, a new phosphate species from Toms quarry, South Australia: description and structural relationship to mélonjosephite. *American Mineralogist*, **95**, 754–760.

Mohaček-Grošev V., Grdadolnik J., Stare J. and Hadži D. (2009) Identification of hydrogen bond modes in polarized Raman spectra of single crystals of α-oxalic acid dihydrate. *Journal of Raman Spectroscopy*, **40**, 1605–1614.

Rudolph W.W. and Irmer G. (2007) Raman and infrared spectroscopic investigations on aqueous alkali metal phosphate solutions and density functional theory calculations of phosphate–water clusters. *Applied Spectroscopy*, **61**, 1312–1327.

Sergeeva A.V., Zhitova E.S and Bocharov V.N. (2019) Infrared and Raman spectroscopy of tschermigite, $\mathrm{(NH_4)Al(SO_4)_2 \cdot 12H_2O}$. *Vibrational Spectroscopy*, **105**, 102983.

Sheldrick G.M. (2015) Crystal structure refinement with SHELX. *Acta Crystallographica*, **C71**, 3–8.

Števko M., Sejkora J., Uher P., Cámara F., Škoda R. and Vaculovič T. (2018) Fluorarrojadite-(BaNa), $\mathrm{BaNa_4CaFe_{13}Al(PO_4)_{11}(PO_3OH)F_2}$, a new member of the arrojadite group from Gemerská Poloma, Slovakia. *Mineralogical Magazine*, **82**, 863–876.

Wilson W.E. (2020) The Rowley mine, Painted Rock Mountains, Maricopa County, Arizona. *Mineralogical Record*, **51**, 181–226.

Yakovenchuk V.N., Pakhomovsky Y.A., Konopleva N.G., Panikorovskii T.L., Bazai A., Mikhailova J.A., Bocharov V.N., Ivanyuk G.Yu. and Krivovichev S.V. (2018) Batagayite, $\mathrm{CaZn_2(Zn,Cu)_6(PO_4)_4(PO_3OH)_3 \cdot 12H_2O}$, a new phosphate mineral from Këster tin deposit (Yakutia, Russia): occurrence and crystal structure. *Mineralogy and Petrology*, **112**, 591–601.